

Beyond the rainbow: effects from pion back-coupling

Christian S. Fischer^{1,2} and Richard Williams¹

¹*Institute for Nuclear Physics, Darmstadt University of Technology,
Schlossgartenstraße 9, 64289 Darmstadt, Germany*

²*Gesellschaft für Schwerionenforschung mbH, Planckstr. 1 D-64291 Darmstadt, Germany.*

(Dated: October 26, 2018)

We investigate hadronic unquenching effects in light quarks and mesons. To this end we take into account the back-coupling of the pion onto the quark propagator within the non-perturbative continuum framework of Schwinger-Dyson equations (SDE) and Bethe-Salpeter equations (BSE). We improve on a previous approach by explicitly solving both the coupled system of DSEs and BSEs in the complex plane and the normalisation problem for Bethe-Salpeter kernels depending on the total momentum of the meson. As a result of our study we find considerable unquenching effects in the spectrum of light pseudoscalar, vector and axial-vector mesons.

PACS numbers: 12.38.Aw, 12.38.Gc, 12.38.Lg, 14.65.Bt

Keywords: Dynamical chiral symmetry breaking, light mesons, pion cloud

I. INTRODUCTION

In hard scattering events mesons and baryons can be viewed as bound states built up from partonic constituents, i.e. quarks and gluons. This picture changes at low energies, where hadronic effects play a more prominent rôle in the nonperturbative structure of hadrons. Of particular importance are pion cloud effects which *e.g.* have a direct impact on the spin structure of the proton [1]. Thus they need to be incorporated in bound-state calculations aiming at a realistic description of mesons and baryons.

For the spectrum of light pseudoscalar mesons, it is the axial-vector Ward-Takahashi identity that governs the pattern of dynamical symmetry breaking, rather than the intricacies of confinement or infrared specifics of QCD. Within the framework of Schwinger-Dyson (SDE) and Bethe-Salpeter (BSE) equations, this realisation has led to much phenomenological success in describing pseudoscalar and vector mesons [2, 3, 4], with bound-state masses, decay constants and electromagnetic form-factors determined [5, 6] with surprising agreement to experiment [7].

The success of this description partly comes from the vector-vector coupling of the rainbow-ladder truncation, where the resultant spin-coupling to these *S*-wave mesons is dominant. For *P*-wave states however, such as the scalar and axial-vector mesons, a richer tensor structure is required from the quark-gluon vertex to properly account for the observed spectrum. To this end, the scalar part of the quark-gluon vertex, whose importance regarding confinement has been highlighted in [8], may be the most relevant for introducing a spin-dependence to the interaction. We expect any beyond-the-rainbow study that generates such terms to have an effect on the spectrum of light mesons.

However, there arise further complications in describing the scalar and axial-vector sector. Not only are models employing the rainbow-ladder truncation too attractive, yielding masses of 800-900 MeV [4, 9], but are these

mesons even $q\bar{q}$ bound states? For the scalars we have tetraquarks, multi-meson molecules, glueballs and the inevitable hybrids as candidates (see *e.g.* [10, 11]). Indeed, these exotics are not restricted to the scalar sector, for the a_1 may be well described as a coupled-channel meson molecule [12], amongst other equally plausible descriptions [13, 14]. Clearly there is much work to be done in providing a dynamical partonic description of these ‘mesons’, not least in understanding the fundamental interactions between quarks and gluons.

As a further step in this direction we concentrate in this work on improving our model description of $\bar{q}q$ bound-states. Based on an approximation scheme for the quark-gluon interaction developed in [15] and [16] we study the pion back-reaction on the quarks and light mesons in the covariant Schwinger-Dyson/Bethe-Salpeter approach to Landau gauge QCD [17, 18]. As a consequence we take into account pion cloud effects in the light meson spectrum. To this end we solve the coupled system of quark Schwinger-Dyson equations and Bethe-Salpeter equations for pseudoscalar, vector and axial-vector mesons in the complex plane. This provides for an important technical progress compared to the calculations in Ref. [15], where the so-called real-value approximation has been used. As a further technical complication we then have to solve the normalisation problem for Bethe-Salpeter amplitudes generated by a kernel depending on the total momentum of the meson.

The paper is organized as follows. In Sec. II. we summarise our approximation scheme for the quark-gluon interaction developed in detail in [15, 16]. We specify our model interaction and discuss the technical complications that appear in the normalisation condition for the bound-state amplitudes. We explicitly verify that our interaction satisfies the axial-vector Ward-Takahashi identity. In Sec. III. we then provide the details of our calculation and present our results. We conclude with an outlook in Sec. IV. Some technical discussions are relegated to an appendix.

part one takes a rainbow-ladder form of the interaction, *i.e.* one chooses a model for the fully dressed Yang-Mills part of the quark-gluon vertex Γ_ν^{YM} of the form

$$\Gamma_\nu^{\text{YM}}(p_1, p_2, p_3) = \gamma_\nu Z_2 / \tilde{Z}_3 \Gamma^{\text{YM}}(p_3^2), \quad (3)$$

where we denote the quark momenta by p_1 and p_2 and the gluon momentum by p_3 . The explicit expression for $\Gamma^{\text{YM}}(p_3^2)$ is detailed below. A similar form has been used in [27, 28], where quenched lattice results for the quark propagator have been reproduced. Note, however, that (3) involves only the γ_ν -part of the tensor structure of the full Yang-Mills part of the vertex. It has been shown in the analysis of the full quark-gluon vertex of Ref. [8] that such a model cannot capture all essentials of dynamical chiral symmetry breaking. Indeed, from the results of this work we will draw the very same conclusion from our calculation of the light meson spectrum.

In general one can decompose the quark-gluon vertex $\Gamma_\nu(p_1, p_2, p_3)$ into 12 different tensor structures, given by

$$\Gamma_\nu(p_1, p_2, p_3) = \sum_{i=1}^{12} \lambda_i(p_1, p_2, p_3) L_\nu^i(p_1, p_2, p_3). \quad (4)$$

The details of this basis are given in Ref. [29]. Here, we only note that $L_\nu^1 = \gamma_\nu$; the explicit forms of the other structures are not needed. In principle, all twelve tensor structures are important in the infrared and intermediate momentum regime [8, 30]. We have verified by projection methods that the pion-exchange diagram in the vertex-SDE indeed contributes to all these structures. Therefore the resulting one-pion contribution in the propagator SDE Fig. 2 generates unquenching effects in all components of the quark-gluon interaction.

An explicit expression for the one pion-exchange kernel that satisfies the axial-vector Ward-Takahashi identity has been constructed in [15]. Here we give a similar construction which takes into account the modifications suggested in [16]. The resulting SDE for the quark propagator is given by

$$\begin{aligned} S^{-1}(p) = & Z_2 S_0^{-1}(p) + g^2 C_F (Z_2)^2 \int \frac{d^4 q}{(2\pi)^4} \gamma_\mu S(q) \gamma_\nu \left(\delta_{\mu\nu} - \frac{k_\mu k_\nu}{k^2} \right) \frac{Z(k^2) \Gamma_{\text{YM}}(k^2)}{k^2} \\ & - 3 \int \frac{d^4 q}{(2\pi)^4} \left[Z_2 \gamma_5 S(q) \Gamma_\pi \left(\frac{p+q}{2}; q-p \right) + Z_2 \gamma_5 S(q) \Gamma_\pi \left(\frac{p+q}{2}; p-q \right) \right] \frac{D_\pi(k^2)}{2} \end{aligned} \quad (5)$$

with $k = p - q$ and $D_\pi(k) = (k^2 + M_\pi^2)^{-1}$ being the pion propagator. The factor 3 in front of the pion contribution stems from the flavour trace and represents contributions from π_+ , π_- and π_0 . These are treated on equal footing

in the isospin-symmetric limit adopted here.

The corresponding expression for the Bethe-Salpeter equation for light mesons reads

$$\Gamma_{tu}^{(\mu)}(p; P) = \int \frac{d^4 k}{(2\pi)^4} \left\{ K_{tu;rs}^{\text{YM}}(p, k; P) + K_{tu;rs}^{\text{pion}}(p, k; P) \right\} \left[S(k_+) \Gamma^{(\mu)}(k; P) S(k_-) \right]_{sr} \quad (6)$$

with the kernels $K_{tu;rs}^{\text{YM}}$ and $K_{tu;rs}^{\text{pion}}$ given by

$$K_{tu;sr}^{\text{YM}}(q, p; P) = \frac{g^2 Z(k^2) \Gamma^{\text{YM}}(k^2) Z_{1F}}{k^2} \left(\delta_{\mu\nu} - \frac{k_\mu k_\nu}{k^2} \right) \left[\frac{\lambda^a}{2} \gamma_\mu \right]_{ts} \left[\frac{\lambda^a}{2} \gamma_\nu \right]_{ru}, \quad (7)$$

$$\begin{aligned} K_{tu;rs}^{\text{pion}}(q, p; P) = & \frac{1}{4} [\Gamma_\pi^j]_{ru} \left(\frac{p+q-P}{2}; p-q \right) [Z_2 \tau^j \gamma_5]_{ts} D_\pi(p-q) \\ & + \frac{1}{4} [\Gamma_\pi^j]_{ru} \left(\frac{p+q-P}{2}; q-p \right) [Z_2 \tau^j \gamma_5]_{ts} D_\pi(p-q) \\ & + \frac{1}{4} [\Gamma_\pi^j]_{ts} \left(\frac{p+q+P}{2}; p-q \right) [Z_2 \tau^j \gamma_5]_{ru} D_\pi(p-q) \\ & + \frac{1}{4} [\Gamma_\pi^j]_{ts} \left(\frac{p+q+P}{2}; q-p \right) [Z_2 \tau^j \gamma_5]_{ru} D_\pi(p-q). \end{aligned} \quad (8)$$

	Component	0 ⁻	0 ⁺
$T_1(p; P) :$	$\mathbb{1}$	○	○
$T_2(p; P) :$	$-i\mathcal{P}$	○	●
$T_3(p; P) :$	$-i\mathcal{P}$	●	○
$T_4(p; P) :$	$[\mathcal{P}, \mathcal{P}]$	○	○

TABLE I: The four Dirac structures describing a meson of spin $J = 0$. For the pseudoscalar, these have an associated factor of γ_5 to account for parity. Circles indicate that the component is part of the basis decomposition of the meson, with filled circles indicating that the component is multiplied by $(p \cdot P)$. This ensures that for equal-mass constituents a Chebyshev decomposition of even order need only been employed for the scalar amplitudes F_i .

	Component	1 ⁻	1 ⁺⁺	1 ⁺⁻
$T_1^\mu(p; P) :$	$i\gamma_T^\mu$	○	○	
$T_2^\mu(p; P) :$	$\gamma_T^\mu \mathcal{P}$	○	●	
$T_3^\mu(p; P) :$	$-\gamma_T^\mu \mathcal{P} + p_T^\mu \mathbb{1}$	●	○	
$T_4^\mu(p; P) :$	$i\gamma_T^\mu [\mathcal{P}, \mathcal{P}] + 2ip_T^\mu \mathcal{P}$	○	○	
$T_5^\mu(p; P) :$	$p_T^\mu \mathbb{1}$	○		○
$T_6^\mu(p; P) :$	$ip_T^\mu \mathcal{P}$	●		○
$T_7^\mu(p; P) :$	$-ip_T^\mu \mathcal{P}$	○		●
$T_8^\mu(p; P) :$	$p_T^\mu [\mathcal{P}, \mathcal{P}]$	○		○

TABLE II: The eight Dirac structures describing a meson of spin $J = 1$. For the axial-vectors, there is an additional factor of γ_5 to account for parity. Circles indicate that the component is included in the basis decomposition of the meson, with filled circles indicating the component is multiplied by $(p \cdot P)$. This ensures that an even Chebyshev decomposition is sufficient for equal-mass constituents. The subscript T indicates transversality with respect to the total momentum.

Here $\Gamma^{(\mu)}(p; P)$ is the Bethe-Salpeter vertex function of a quark-antiquark bound state specified below, whereas Γ_π^j with flavour index j is the corresponding vertex function of a pion. The momenta $k_+ = k + P/2$ and $k_- = k - P/2$ are such that the total momentum P of the meson is given by $P = k_+ - k_-$ and the relative momentum $k = (k_+ + k_-)/2$. The Latin indices (t, u, r, s) of the kernels refer to colour, flavour and Dirac structure.

The Bethe-Salpeter vertex function $\Gamma(p; P)^{(\mu)}$ can be decomposed into at most eight Lorentz and Dirac structures. The structure is constrained by the transformation properties under CPT of the meson we wish to describe [31]. In particular, our pseudoscalar, scalar and vector have quantum numbers J^P of 0^- , 0^+ and 1^- , respectively. The axial-vector can be parameterised in two different ways, dependent on its transformation under charge conjugation, $J^{PC} = 1^{++}$ and 1^{+-} .

Taking this into consideration, we can write down a

general basis for each desired meson amplitude,

$$\Gamma_M^{(\mu)}(p; P) = \begin{cases} \sum_i F_i(p; P) T_i^{(\mu)}(p; P) & J^P = 0^+, 1^- \\ \sum_i \gamma_5 F_i(p; P) T_i^{(\mu)}(p; P) & J^P = 0^-, 1^+ \end{cases} \quad (9)$$

where the components $T_i^{(\mu)}$ are given in Tables I and II.

In particular, the pion is given by the following form

$$\Gamma_\pi(p; P) = \gamma_5 \left[F_1(p; P) - i\mathcal{P} F_2(p; P) - i\mathcal{P} (p \cdot P) F_3(p; P) - [\mathcal{P}, \mathcal{P}] F_4(p; P) \right]. \quad (10)$$

B. Model details

Next we need to specify the details of our model interaction. For the Yang-Mills part of the interaction we choose two different model ansätze that have been employed already in previous works. Here, the gluon dressing function $Z(k^2)$ from (2) and the Yang-Mills part $\Gamma^{\text{YM}}(k^2)$ of the quark-gluon vertex Eq. (3) are combined and represented by a single function. For the Maris-Tandy (MT) model [4] this function is given by

$$Z(k^2) \Gamma^{\text{YM}}(k^2) = \frac{4\pi}{g^2} \left(\frac{\pi}{\omega^6} D q^4 \exp(-q^2/\omega^2) + \frac{2\pi\gamma_m}{\log \left(\tau + \left(1 + q^2/\Lambda_{\text{QCD}}^2 \right)^2 \right)} \times [1 - \exp(-q^2/[4m_t^2])] \right), \quad (11)$$

with

$$m_t = 0.5 \text{ GeV}, \quad \tau = e^2 - 1 \\ \gamma_m = 12/(33 - 2N_f), \quad \Lambda_{\text{QCD}} = 0.234 \text{ GeV}.$$

This model has been employed successfully in various calculations of meson spectra, form factors and decay constant within a rainbow-ladder truncation; see [17, 22] for overviews of the results. The remaining parameters D , ω and the quark mass are fitted to pion observables, and detailed in Sec. III.

The second model we employ for the Yang-Mills part of the quark-gluon interaction represents the infrared structure of both the gluon dressing function $Z(k^2)$ and the quark-gluon vertex $\Gamma^{\text{YM}}(k^2)$, in quenched approximation (up to effects due to hairpin diagrams) as calculated in Refs. [8, 32]. It has been used to show that infrared divergences in vertex functions can account for the topological

mass of the η' -meson [33], and is given by

$$\begin{aligned}
 Z(k^2) &= \left(\frac{k^2}{k^2 + \Lambda_{\text{QCD}}^2} \right)^{2\kappa} \left(\frac{\alpha_{\text{fit}}(k^2)}{\alpha_\mu} \right)^{-\gamma}, \\
 \Gamma^{\text{YM}}(k^2) &= \left(\frac{k^2}{k^2 + d_2} \right)^{-1/2-\kappa} \\
 &\times \left(\frac{d_1}{d_2 + k^2} + \frac{k^2 d_3}{d_2^2 + (k^2 - d_2)^2} + \frac{k^2}{\Lambda_{\text{QCD}}^2 + k^2} \right. \\
 &\times \left. \left[\frac{4\pi}{\beta_0 \alpha_\mu} \left(\frac{1}{\log\left(\frac{k^2}{\Lambda_{\text{QCD}}^2}\right)} - \frac{\Lambda_{\text{QCD}}^2}{k^2 - \Lambda_{\text{QCD}}^2} \right) \right]^{-2\delta} \right)
 \end{aligned} \quad (12)$$

with the gluon momentum k^2 , the one-loop value $\gamma = (-13N_c + 4N_f)/(22N_c - 4N_f)$ for the anomalous dimension of the re-summed gluon propagator, the corresponding one $\delta = \frac{-9N_c}{44N_c - 8N_f}$ for the ghost dressing function and $\alpha_\mu = 0.2$ at the renormalisation scale $\mu^2 = 170 \text{ GeV}^2$. We use $\Lambda_{\text{QCD}}^2 = 0.52 \text{ GeV}^2$ similar to the scale obtained in Ref. [32]. The infrared exponent κ has been determined analytically in [34, 35] and is given by $\kappa = (93 - \sqrt{1201})/98 \simeq 0.595$. Note that this form is slightly modified to that reported in [16, 33], allowing more freedom in separating the scales in the quark-gluon vertex and the gluon propagator. The parameter d_1 sets the strength of the interaction in the infrared. The parameters d_2 and d_3 determine the location and size of a term added to give additional integrated strength in the intermediate momentum regions. These three parameters, together with the current quark mass, are constrained by pion observables and the generation of a topological charge in the pseudoscalar isosinglet channel. The running coupling from the ghost-gluon vertex, $\alpha_{\text{fit}}(p^2)$, is parameterised such that the numerical results for Euclidean scales are accurately reproduced [32]:

$$\begin{aligned}
 \alpha_{\text{fit}}(p^2) &= \frac{\alpha_s(0)}{1 + p^2/\Lambda_{\text{QCD}}^2} + \frac{4\pi}{\beta_0} \frac{p^2}{\Lambda_{\text{QCD}}^2 + p^2} \\
 &\times \left(\frac{1}{\ln(p^2/\Lambda_{\text{QCD}}^2)} - \frac{1}{p^2/\Lambda_{\text{QCD}}^2 - 1} \right).
 \end{aligned} \quad (13)$$

Here $\beta_0 = (11N_c - 2N_f)/3$, and $\alpha_s(0)$ is the fixed point in the infrared, calculated to be $\alpha_s(0) = 8.915/N_c$ for our choice of κ . In this work, we will take $N_f = 2$.

The resulting two effective interactions from the Maris-Tandy model (11) and our soft-divergence model (12) are plotted against each other in Fig. 4. The ultraviolet running of both interactions are the same except for differences in the scale employed. Whereas the Maris-Tandy model used a scale corresponding to the $\overline{\text{MS}}$ scheme, we are working in a momentum subtraction scheme where the scale is larger by more than a factor of 3. Both interactions share an enhancement in the intermediate momentum region which provides the necessary interaction strength for dynamical chiral symmetry breaking. The

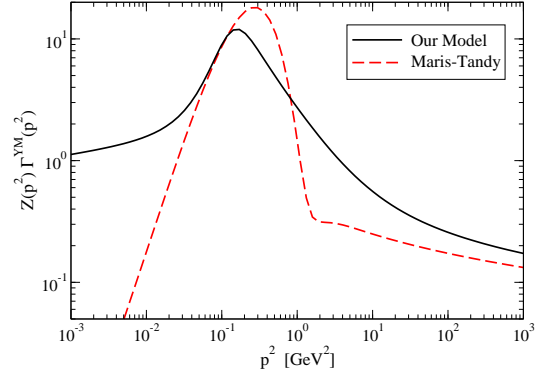


FIG. 4: A log-log plot of the effective quark-gluon interaction $Z\Gamma^{\text{YM}}$ for the two models we employ. Differences in the UV behaviour are attributed to the different scale Λ_{QCD}^2 in use. Note both exhibit enhancement in the intermediate momentum region.

change of slope in the infrared region of our interaction is related to the topological mass component of the η' in the chiral limit [33].

As for the pion part of our interaction, we approximate the full pion Bethe-Salpeter wave function (10) in the quark-SDE (5) and the kernel of the BSE (8) by the leading amplitude in the chiral limit given by [2]

$$\Gamma_\pi^j(p; P) = \tau^j \gamma_5 \frac{B(p^2)}{f_\pi}. \quad (14)$$

Here $B(p^2)$ is the scalar dressing function of the quark propagator in the chiral limit. This approximation omits the back-coupling effects of the three sub-leading amplitudes. From the calculation of ref. [15], where full back-coupling has been evaluated in a real value approximation, we expect this omission to lead to an error of only a few percent as concerns meson masses and of about 10-20% as concerns decay constants. Considering the exploratory character of our work this seems certainly tolerable. The replacement of the leading physical pion amplitude $F_1(p; P)$ at $m_\pi = 138 \text{ MeV}$ by the (normalised) chiral limit value $F_1(p; P) \approx \frac{B(p^2)}{f_\pi}$ is also correct on the few percent level as demonstrated in the appendix. Note that we use this approximation only for the internal pion which mediates the interaction. The great advantage of the approximation (14) compared to the full back-coupling performed in Ref. [15] is that we can then fully take into account the quark propagator in the complex plane as necessary input into the Bethe-Salpeter equation.

C. Decay constants and normalisation

The Bethe-Salpeter amplitudes for the pseudoscalar mesons can be used to obtain the corresponding weak decay constants f_π , which will prove useful in fitting parameters to observables. In order to calculate these one

must firstly normalise the amplitudes. The normalisation condition is derived by demanding that the residue of the pole in the four-point quark-antiquark Green's function (from which the BSE is derived) be unity [36, 37]. Using conventions such that $f_\pi = 93$ MeV, and for momenta partitioned equally between the two constituents, it reads

$$\delta^{ij} = 2 \frac{\partial}{\partial P^2} \text{tr} \int \frac{d^4 k}{(2\pi)^4} \left[3 \left(\bar{\Gamma}_\pi^i(k, -Q) S(k + P/2) \Gamma_\pi^j(k, Q) S(k - P/2) \right) + \int \frac{d^4 q}{(2\pi)^4} [\bar{\chi}_\pi^i]_{sr}(q, -Q) K_{tu;rs}^{\text{pion}}(q, k; P) [\chi_\pi^j]_{ut}(k, Q) \right], \quad (15)$$

where $Q^2 = -M^2$ is fixed to the on-shell meson mass, the trace is over Dirac matrices and the Bethe-Salpeter wave-function χ is defined by

$$\chi_\pi^j(k; P) = S(k + P/2) \Gamma_\pi^j(k, P) S(k - P/2). \quad (16)$$

The conjugate vertex function $\bar{\Gamma}$ is given by

$$\bar{\Gamma}(p, -P) = C \Gamma^T(-p, -P) C^{-1}, \quad (17)$$

with the charge conjugation matrix $C = -\gamma_2 \gamma_4$. The leptonic decay constant characterising the pion coupling to the point axial field is subsequently given by [37]

$$f_\pi = Z_2 \frac{3}{M^2} \text{tr} \int \frac{d^4 k}{(2\pi)^4} \Gamma_\pi(k, -P) S(k_+) \gamma_5 \not{P} S(k_-), \quad (18)$$

where again the trace is over Dirac matrices, and $k_+ = k + P/2$, $k_- = k - P/2$. There exist analogous expressions for the vector mesons [4], where an additional factor of 1/3 must be included due to summation over the polarisation tensor.

One may write a similar equation to (18), which corresponds to the residue of the pseudoscalar vertex:

$$r_\pi = Z_2 Z_m 3 \text{tr} \int \frac{d^4 k}{(2\pi)^4} \Gamma_\pi(k, -P) S(k_+) \gamma_5 S(k_-). \quad (19)$$

The axWTI imposes a relationship between these two residues, known as the generalised Gell-Mann–Oakes–Renner relation [3], which must hold at and beyond the chiral limit:

$$f_\pi m_\pi^2 = r_\pi (m_u(\mu^2) + m_d(\mu^2)), \quad (20)$$

where m_u , m_d are the masses of the up and down quarks at the renormalisation point μ^2 , and in this work considered to be degenerate. Confirming this relation serves as a check of both our numerics and indicates how well our kernel satisfies the axWTI. We find excellent agreement with errors smaller than 1% for pion masses up to $m_\pi \simeq 600$ MeV.

III. NUMERICAL METHODS AND RESULTS

A. Solving the BSE

We solve the BSE for the meson amplitude $\Gamma^{(\mu)}(p; P)$ via matrix methods using the following procedure. First, we project our BSE onto the scalar amplitudes of our meson decomposition. This gives rise to either four or eight coupled integral equations for the $F_i(p; P)$. To make manifest the angular dependence of the amplitude functions, we treat the total momentum P^2 as a parameter and expand the function as a series of Chebyshev polynomials in the angle $\widehat{p \cdot P} = p \cdot P / |pP|$

$$F_i(p; P) = \sum_k (i)^k F_i^k(p^2; P^2) T_k(\widehat{p \cdot P}). \quad (21)$$

The functions $F_i^k(p^2; P^2)$ are projected out through use of the orthonormal properties of the Chebyshev polynomials. With the angular dependence made explicit, we can evaluate numerically the two non-trivial angles appearing in the integration measure. We cast the remaining radial integral in the form of a matrix equation by matching the external momenta to the radial loop momenta, $p_j^2 = k_j^2$ at the abscissae of our integration nodes. Thus the amplitude of our BS equation is projected onto the decomposition $F_i^k(p_j^2; P^2)$. Schematically we are solving

$$\Gamma = \lambda \mathbf{K} \cdot \Gamma, \quad (22)$$

for the column vector Γ as a parametric equation in $P^2 = -M^2$ with M the mass of the meson. A bound-state corresponds to solutions with $\lambda = 1$, which as an eigenvalue problem is equivalent to satisfying the condition $\det(1 - \mathbf{K}) = 0$. Because of the tractable nature of our unquenching prescription, the computational effort required to determine the Bethe-Salpeter amplitude increases from a few seconds to a few minutes. However, we see in the next section that substantial effort is required to calculate the normalisation condition with any kernel involving momentum exchange of the meson.

B. Calculating the normalisation

The first term of (15), independent of the kernel, is easily evaluated since the quark propagator derivatives are directly calculable in our approach; either by applying the derivative to the quark-SDE, and solving the resulting integral equation, or by finite difference methods. The second term is substantially more complicated for two reasons. First, we must determine the derivative of our exchange kernel with respect to the total momentum dependence – a tractable but algebraically complicated task. The second problem is the double integration over two four-momenta, k and q . Decomposing the measure into hyperspherical coordinates, where none of the angles

may be evaluated trivially, results in the need to evaluate an eight dimensional integral numerically. Resigning ourselves to this computationally intensive task, we evaluate the integral of (15) for $P^2 = Q^2 \pm 2^n \Delta$, and employ the appropriate Richardson improved centered difference formula. Typically, we use a four-point rule for which $n = 0, 1$ though a two-point rule is sufficient, provided we choose Δ optimally. Unfortunately each double integral must still be evaluated, which we tackled using both Monte-Carlo and Gaussian quadrature techniques. For the latter, a small-scale computing cluster is mandatory for even moderate grid sizes. Monte-Carlo performs only marginally better in terms of necessary computing time, since the statistical errors must be minimised such that the numerical derivative is meaningful. With due care, however, both methods obviously yield the same result.

In the next section, we give results for the leptonic decay constants for the pion and rho with and without consideration of the normalisation double-integral. For a physical pion, the difference is only about 3% and smaller still for the rho. However, as we reduce the pion mass and approach the chiral limit the necessity of including the full normalisation condition becomes readily apparent.

C. Results

The parameters of the two models we employed – that of Maris-Tandy and our model – were tuned such that pion observables were well reproduced with the inclusion of the hadronic exchange kernel. For our interaction, which is capable of generating a topological charge, the eta/eta' splitting provides an additional constraint.

For the Maris-Tandy model, we find a unique choice of ω and D for a given quark mass by fitting to m_π and f_π . We attempted to maximise the rho meson mass, though we did not exhaust the available parameter space due to the complexity in evaluating the full normalisation condition. Consequently we employ $\omega = 0.37$ GeV and $D = 1.45$ GeV², with a quark mass of 3.7 MeV at $\mu = 19$ GeV.

The parameters of our model interaction were fit in a similar fashion, with the additional step of calculating the topological charge for each parameter set. As a result, we obtained good agreement with experiment with the choice $d_1 = 1.45$ GeV², $d_2 = 0.1$ GeV² and $d_3 = 3.95$ GeV². Here we choose a quark mass $m(\mu) = 2.6$ MeV defined at the renormalisation point $\mu^2 = 170$ GeV².

In Table III, we present a summary of meson observables calculated for these two interactions, with and without the inclusion of the pion exchange kernel. One may then compare the effects of unquenching for two models with dissimilar behaviour in the infrared and intermediate momentum regions (see Fig. 4). Though the details of the deep infrared are generally unimportant for the pattern of dynamical symmetry breaking in light mesons, we expect a complicated interplay from the dynamics

	Maris-Tandy		Our Model		Experiment (PDG [38])
	w/o pi	incl. pi	w/o pi	incl. pi	
M_π	140	138 [†]	125	138 [†]	138
f_π	104	93.2 [†] (90.2)	102	93.8 [†] (90.6)	92.4
M_σ	746	598	638	485	400 – 1200
M_ρ	821	720	795	703	776
f_ρ	160	167 (167)	159	162 (165)	156
M_{a_1}	979	913	941	873	1230
M_{b_1}	820	750	879	806	1230
M_η			493	497	548
$M_{\eta'}$			949	963	948

TABLE III: BSE results for the pseudoscalar, scalar, vector and axial-vector mesons for the Maris-Tandy and soft-divergence models employed with ('incl.') and without ('w/o') pion backreaction. The parameters marked by [†] are fitted to reproduce the pion mass and decay constant when the pion-exchange kernel is switched on. Consequently the model parameters, given in the text, are modified compared to the original Maris-Tandy model [4]. Results for the pure rainbow-ladder kernel without pion back-reaction are for the same parameter set. Decay constants given in parenthesis are those that would result without calculating the full normalisation condition of the appropriate meson.

present in any beyond-the-rainbow truncation.

This difference in the two interactions is seen most prominently for the pion. Though the effects here are small, as to be expected we see immediately a difference for the two models. Whilst for Maris-Tandy, the inclusion of pion-exchange is attractive giving rise to a 2 MeV shift, our model exhibits repulsion of the order of 13 MeV. The leptonic decay constants see a decrease of 10% for both models. The effect of including hadronic contributions is not then *a priori* known, at least for those mesons most sensitive to dynamical chiral symmetry breaking.

For the remaining light mesons, the inclusion of the pion back-reaction generally leads to a lighter spectrum. In the case of the scalar meson, we see a reduction of 150 MeV for both interactions, though the relative drop is significantly different at 20 and 40% for Maris-Tandy and our model respectively.

The vector meson - here identified with the ρ - receives a negative shift of 100 MeV, or 12% for both interactions. In the case of Maris-Tandy, the resultant rho mass of ~ 720 MeV is similar to that obtained in other studies with this interaction [4]. Here, unquenching has the effect of increasing the decay constant by 5%. Our interaction yields a lighter mass of around 700 MeV, with unquenching increasing the decay constant by just 2%. Since our truncation scheme does not provide a mechanism for the ρ to decay into pions, we do not observe the tell-tale non-analytic behaviour of the rho mass as a function of the pion mass, due to the opening of a decay channel, as shown in Ref. [39].

Next, we examine the axial-vectors a_1 and b_1 , which differ by their charge conjugate properties. As already seen, the net effect of including the pion back-reaction is a reduction in the meson mass. For the axial-vectors, we see a 70 MeV reduction in the bound-state mass for both charge eigenstates and in both models of the interaction. It is evident, at least with our tractable unquenching truncation scheme, that unquenching effects do not resolve the difficulties we have in obtaining reasonable masses for these mesons. However, we note that the anomalous mass-splitting in calculations of the a_1 and b_1 in our model is half that of Maris-Tandy. In the course of our investigations of possible parameter sets, we could easily obtain near degenerate axial-vector masses within our interaction.

Finally, we take a look at the masses of the η and η' . For our model, which exhibits a soft-divergence in the gluon momentum, we calculate a non-zero topological mass following Ref. [33]. We see that the inclusion of the pion back-reaction on the quark propagator has a minimal effect on the phenomenologically determined mass-splittings.

IV. CONCLUSIONS AND OUTLOOK

Using an approximation scheme for including pion loop effects in the quark-gluon interaction, we investigated effects of the pion cloud in the Bethe-Salpeter and Schwinger-Dyson equations. By considering only the leading amplitude of the exchange pion, moreover taken from its chiral limit solution, we were able to include the analytic behaviour beyond the real-value approximation employed in the previous study [15]. The resulting interaction respects the axial-vector Ward-Takahashi identity.

As a consequence of this technical improvement, we were forced to tackle the added complication of calculating the full normalisation condition of the Bethe-Salpeter equation where the momentum exchange of the kernel need be considered. We found that this indeed gives a sizable contribution of the order of a few percent that must be properly taken into account in order to extract the correct leptonic decay constants.

As a result, we found considerable pion cloud effects in the spectrum of light mesons. In particular we found a shift of about 100 MeV for the mass of the rho-meson in agreement with expectations from chiral extrapolations of quenched lattice data [40].

Though this truncation scheme represents a tractable model for including hadronic unquenching effects, it is

clear that spin dependent contributions from the Yang-Mills part of the quark-gluon vertex will have a strong impact upon the spectrum of light mesons. Such corrections will form a part of future investigations.

Acknowledgements

We are grateful to Michael Buballa and Dominik Nickel for fruitful discussions on the pion back-reaction. We thank Peter Tandy for a critical reading of the manuscript. This work has been supported by the Helmholtz-University Young Investigator Grant No. VH-NG-332.

APPENDIX A: PION AMPLITUDE AT AND AWAY FROM THE CHIRAL LIMIT

One of the key approximations here is that the leading Bethe-Salpeter amplitude for the pion may be well approximated by the chiral limit result B/f_π . It is important for the amplitude to feature the correct asymptotic behaviour at large momenta, and so for a massive pion in the exchange kernel we employ the scalar self-energy B as calculated in the chiral limit (for complex momenta). The differences between this and the full amplitude are shown in Fig. 5 and are seen to be at the level of a few percent.

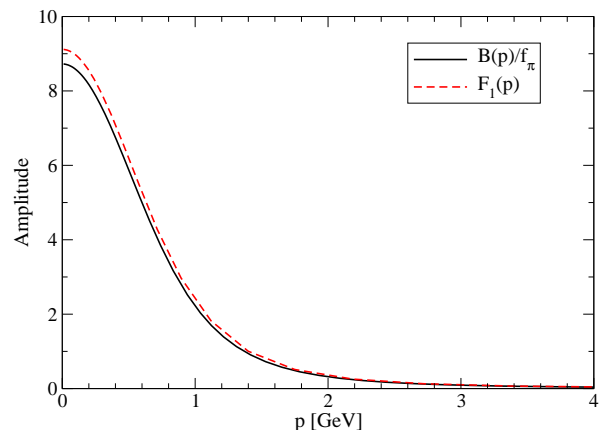


FIG. 5: The leading physical pion amplitude $F_1(p, P)$ at $m_\pi = 138$ MeV, compared to the normalised chiral limit value $F_1(p; P) \approx \frac{B(p^2)}{f_\pi}$. The angular dependence of this amplitude is negligible, and chosen here such that $(p \cdot P) = 0$.

-
- [1] A. W. Thomas and J. Lab, Prog. Part. Nucl. Phys. **61** (2008) 219 [arXiv:0805.4437 [hep-ph]].
 - [2] P. Maris, C. D. Roberts and P. C. Tandy, Phys. Lett. B **420** (1998) 267 [arXiv:nucl-th/9707003].
 - [3] P. Maris and C. D. Roberts, Phys. Rev. C **56** (1997) 3369

- [arXiv:nucl-th/9708029].
- [4] P. Maris and P. C. Tandy, Phys. Rev. C **60** (1999) 055214 [arXiv:nucl-th/9905056].
- [5] P. Maris and P. C. Tandy, Phys. Rev. C **62**, 055204 (2000) [arXiv:nucl-th/0005015].

- [6] M. S. Bhagwat and P. Maris, Phys. Rev. C **77** (2008) 025203 [arXiv:nucl-th/0612069].
- [7] J. Volmer *et al.* [The Jefferson Lab F(pi) Collaboration], Phys. Rev. Lett. **86**, 1713 (2001) [arXiv:nucl-ex/0010009].
- [8] R. Alkofer, C. S. Fischer and F. J. Llanes-Estrada, Mod. Phys. Lett. A **23**, 1105 (2008) [arXiv:hep-ph/0607293].; R. Alkofer, C. S. Fischer, F. J. Llanes-Estrada and K. Schwenzer, Annals of Physics in print; arXiv:0804.3042 [hep-ph].
- [9] R. Alkofer, P. Watson and H. Weigel, Phys. Rev. D **65** (2002) 094026 [arXiv:hep-ph/0202053].
- [10] C. Amsler and N. A. Tornqvist, Phys. Rept. **389** (2004) 61.
- [11] M. R. Pennington, Int. J. Mod. Phys. A **21** (2006) 747 [arXiv:hep-ph/0509265].
- [12] M. Wagner and S. Leupold, Phys. Rev. D **78** (2008) 053001 [arXiv:0801.0814 [hep-ph]].
- [13] J. A. Oller and E. Oset, Nucl. Phys. A **620** (1997) 438 [Erratum-ibid. A **652** (1999) 407] [arXiv:hep-ph/9702314].
- [14] J. A. Oller and E. Oset, Phys. Rev. D **60** (1999) 074023 [arXiv:hep-ph/9809337].
- [15] C. S. Fischer, D. Nickel and J. Wambach, Phys. Rev. D **76** (2007) 094009 [arXiv:0705.4407 [hep-ph]].
- [16] C. S. Fischer, D. Nickel and R. Williams, arXiv:0807.3486 [hep-ph].
- [17] P. Maris and C. D. Roberts, Int. J. Mod. Phys. E **12** (2003) 297 [arXiv:nucl-th/0301049].
- [18] C. S. Fischer, J. Phys. G **32**, R253 (2006) [arXiv:hep-ph/0605173].
- [19] C. S. Fischer, P. Watson and W. Cassing, Phys. Rev. D **72**, 094025 (2005) [arXiv:hep-ph/0509213].
- [20] P. Watson, W. Cassing and P. C. Tandy, Few Body Syst. **35** (2004) 129 [arXiv:hep-ph/0406340].
- [21] M. S. Bhagwat, A. Holl, A. Krassnigg, C. D. Roberts and P. C. Tandy, Phys. Rev. C **70**, 035205 (2004) [arXiv:nucl-th/0403012].
- [22] P. Maris and P. C. Tandy, Nucl. Phys. Proc. Suppl. **161**, 136 (2006) [arXiv:nucl-th/0511017].
- [23] A. Bender, C. D. Roberts and L. Von Smekal, Phys. Lett. B **380**, 7 (1996) [arXiv:nucl-th/9602012].
- [24] H. H. Matevosyan, A. W. Thomas and P. C. Tandy, Phys. Rev. C **75** (2007) 045201 [arXiv:nucl-th/0605057].
- [25] P. Watson and W. Cassing, Few Body Syst. **35** (2004) 99 [arXiv:hep-ph/0405287].
- [26] C. S. Fischer and R. Alkofer, Phys. Rev. D **67** (2003) 094020 [arXiv:hep-ph/0301094].
- [27] M. S. Bhagwat, M. A. Pichowsky, C. D. Roberts and P. C. Tandy, Phys. Rev. C **68** (2003) 015203 [arXiv:nucl-th/0304003].
- [28] C. S. Fischer and M. R. Pennington, Phys. Rev. D **73** (2006) 034029 [arXiv:hep-ph/0512233]; Eur. Phys. J. A **31** (2007) 746 [arXiv:hep-ph/0701123].
- [29] J. Skullerud and A. Kizilersu, JHEP **0209** (2002) 013 [arXiv:hep-ph/0205318].
- [30] J. I. Skullerud, P. O. Bowman, A. Kizilersu, D. B. Leinweber and A. G. Williams, JHEP **0304** (2003) 047 [arXiv:hep-ph/0303176]; A. Kizilersu, D. B. Leinweber, J. I. Skullerud and A. G. Williams, Eur. Phys. J. C **50** (2007) 871 [arXiv:hep-lat/0610078].
- [31] C. H. Llewellyn-Smith, Annals Phys. **53** (1969) 521.
- [32] R. Alkofer, W. Detmold, C. S. Fischer and P. Maris, Phys. Rev. D **70** (2004) 014014 [arXiv:hep-ph/0309077].
- [33] R. Alkofer, C. S. Fischer and R. Williams, arXiv:0804.3478 [hep-ph].
- [34] D. Zwanziger, Phys. Rev. D **65**, 094039 (2002) [arXiv:hep-th/0109224].
- [35] C. Lerche and L. von Smekal, Phys. Rev. D **65**, 125006 (2002) [arXiv:hep-ph/0202194].
- [36] N. Nakanishi, Prog. Theor. Phys. Suppl. **43** (1969) 1.
- [37] P. C. Tandy, Prog. Part. Nucl. Phys. **39** (1997) 117 [arXiv:nucl-th/9705018].
- [38] W. M. Yao *et al.* [Particle Data Group], J. Phys. G **33** (2006) 1.
- [39] C. R. Allton, W. Armour, D. B. Leinweber, A. W. Thomas and R. D. Young, Phys. Lett. B **628** (2005) 125 [arXiv:hep-lat/0504022].
- [40] D. Leinweber *et al.*, Talk given at the conference 'Tropical QCD' in Port Douglas, Australia, 27.7.-1.8.2008.